Range-rate tradeoffs in the communication between LED traffic lights and vehicles

Jinguo Quan (权进国)[1,2*], Weihao Liu (刘维浩)[2], Shuang Jin (金 爽)[2], and Yan Zhang (张 岩)[1]

[1] *Key Laboratory of Network Oriented Intelligent Computation, Shenzhen Graduate School, Harbin Institute of Technology, Shenzhen 518055, China*

[2] *Division of Information Science and Technology, Shenzhen Graduate School, Tsinghua University, Shenzhen 518055, China*

[*] *Corresponding author: quanjg@gmail.com*

Received June 3, 2013; accepted August 2, 2013; posted online September 29, 2013

Visible light communication between light emitting diode (LED) traffic lights and vehicles with a receiving photodiode front-end is developed for intelligent transportation systems. In this letter, the communication data rates for different ranges are evaluated. The data rates are based on real scenarios of the background noise and path losses and are experimentally obtained with a testing system built upon commercial off-the-shelf components. Comparisons of range-rate performance for different average noise levels are also conducted with the use of red/yellow/green LED lights. Results show that achieving the data rates of kilobits per second at a communication range of hundred meters is possible under the ordinary noise scenario, a finding that is highly significant for practical applications.

OCIS codes: 220.0220, 350.0350.

doi: 10.3788/COL201311.102201.

As fourth generation light sources, light emitting diodes (LEDs) have gained increasing popularity in a variety of applications from lighting to traffic signaling. LEDs have shown superiority over traditional incandescent and fluorescent lamps. LEDs have high energy efficiency, long life expectancy, little out-of-visible band optical radiation, and easy maintenance. They are also environmentally friendly. Nowadays, traditional incandescent traffic light lamps have been increasingly replaced by LED light sources.

Besides the advantages of lighting, LED can also be modulated by input signals because of their semiconductor property that is ideal for information transmission in outdoor vehicle communications. Since the visible light communication (VLC) between LED traffic lights and vehicles has been proposed for intelligent transportation systems[1−3], extensive efforts have been made for traffic light-vehicle VLC based on either photodiode detectors[4−6] or image sensor detectors[7,8]. Image sensors are generally capable of parallel transmission and robustness against interfering light, whereas photodiode sensors have large modulation bandwidth and less response time. Researchers from Nagoya University performed experiments to demonstrate the excellent LED tracking capability of photodiode-based systems[4]. However, data from field experiments on the path loss and background noise of photodiode-based traffic light-vehicle VLC systems under practical scenarios remain insufficient. Systematic analyses based on empirical results are also lacking.

In this letter, we conduct field experimental measurement of real solar radiation noise and path loss in a photodiode-based traffic light–vehicle VLC system. Basing from the experimental results, we further examine the range-rate performance of a communication system built upon commercial off-the-shelf components. The range-rate performance is investigated to understand the communication capability of a photodiode-based outdoor VLC system. The results obtained from this study will be highly significant for practical applications.

Figure 1 shows the general block diagram used in the experimental measurement. To obtain the background noise interference and line of sight (LOS) path loss under real scenarios, the experimental setups are rearranged accordingly.

To measure background noise, the transmitter part is removed from the system, as shown in Fig. 1. The receiver demodulation part is replaced by measurement devices, which include a power meter and a spectrum analyzer. In this way, both optical power and frequency spectrum of the background interfering light are empirically obtained.

To measure path loss, a signal generator with constant signal amplitude replaces the transmitter modulation and combines with the DC bias to drive the LED traffic light lamp. In the receiver side, the spectrum analyzer records the received signal. The carrier to noise density ratio of the receiver is therefore determined when the transmitted signal is a sine wave with a single frequency $\sin(\omega_0 t + \phi)$. Then, the path loss can be obtained from the transmitted signal power and noise intensity.

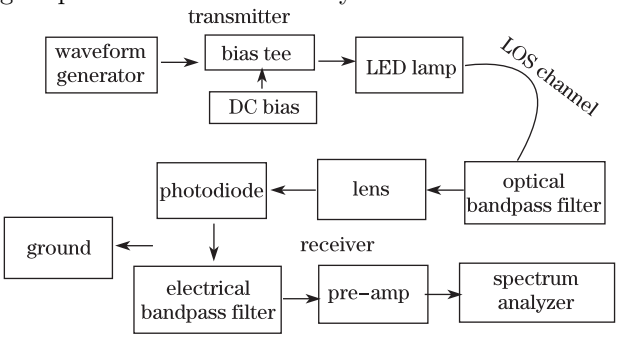

Fig. 1. Block diagram of the experimental measurement.

In real situations, the background noise mainly consists of background solar radiation and radiation from artificial light sources. Because these artificial light sources are largely dependent on the scenario, and quantifying their effects on general communication systems is difficult, we only consider the background interference from solar radiation, which is primarily composed of direct vertical irradiance. A series of factors, such as time, location, weather condition, active receiver area, and receiver field-of-view (FOV), affects the measurement results.

Using a photodiode receiving front-end with an active receiving area of 1 cm^2 and FOV of 15°, we measured the background solar radiations on three typical weather days (sunny, cloudy, and overcast) in Shenzen during December. Figure 2 shows the received power intensity within a day for the case photodiode detector directly pointing to the sun. The received power intensity is obtained by an optical bandpass filter centered at 500 nm (corresponding to green light). Despite some remarkable spikes for the cloudy day, the received vertical power can be largely fitted by a parabola curve with function:

$$S = -0.069T^2 + 1.8062T - 9.5337, \tag{1}$$

where T is the absolute time within a day with the unit "hour". The remarkable spikes are caused by irregular cloud movements.

We adopt an indirect method to obtain the path loss. We first use a spectrum analyzer to determine the carrier to noise density ratio (C/N_0) at night (without environmental noise) when a sine wave source with frequency of 100 kHz is present. Basing from the preamplifier noise specification from the datasheet of the vendor and the responsivity of the detector, we identify the received signal optical power (from C/N_0). The path loss can then be obtained because the total transmitted power can be measured by the power meter. The TRF108-0BG-012V LED traffic light lamp without the plastic cover is used in our measurement. The height of the traffic light is set to 3 m. The horizontal separation between the transmitter and the receiver changes from 5 to 80 m.

The obtained path loss in decibels is shown in Fig. 3. When the range is within 10 m, the path loss shows an edge effect of the LED beam profile. When the range is beyond 10 m, the path loss is properly approximated with the theoretical path loss model[9]. The theoretical path loss model can be described as

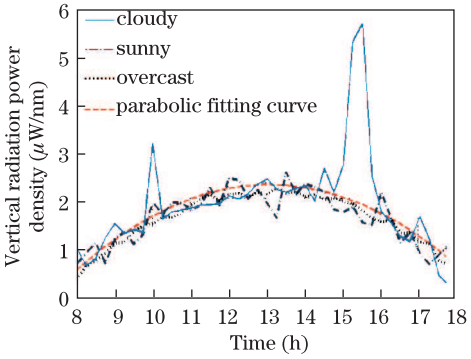

Fig. 2. (Color online) Measured vertical solar power density versus time.

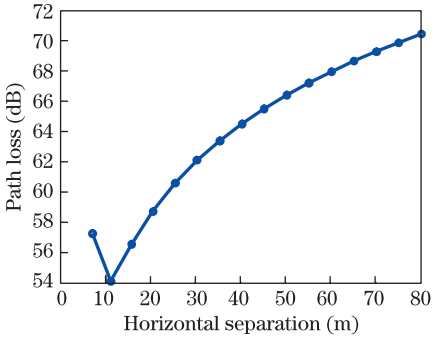

Fig. 3. Measured path loss in dB ($-10\lg P_\mathrm{r}/P_\mathrm{t}$) versus range.

$$L_\mathrm{L} = \frac{P_\mathrm{r}}{P_\mathrm{t}} \approx \frac{g_\mathrm{s}(\beta) A_\mathrm{r} \cos\alpha}{D^2 \int_0^{\theta_\mathrm{max}} 2\pi g_\mathrm{s}(\theta) \sin\theta \mathrm{d}\theta}, \tag{2}$$

where P_r is the received power, P_t is the transmitted power, A_r is the receiving area, α is the receiving angle, θ is the irradiance angle, D is the horizontal distance, $g_\mathrm{s}(\beta)$ is the function dependent on the transmission distance, and β is the transmission angle.

Equation (2) shows that the path loss is determined by both the beam pattern and the transmission distance of the LED traffic light. When the value of D is large enough, transmission angle β shows little variation with D, a result which means that $g_\mathrm{s}(\beta)$ is almost a constant. Equation (2) can therefore be simplified as

$$L_\mathrm{L} \approx \frac{C}{D^2}, \tag{3}$$

where C is a constant. In the following sections, we use these relations to estimate the path loss when the horizontal distance is beyond 80 m.

The communication performance of the system under different practical conditions is evaluated on the basis of the measurement results and empirical models. Table 1 lists the parameters used in the performance evaluation.

The typical noise sources in the practical system include the shot noise σ^2_shot, which is induced by the background solar radiation, and the preamplifier noise σ^2_amp. We assume that the shot noise induced in DC photocurrent is filtered out by an electrical high pass filter. If we consider the on-off keying with Manchester coding as the modulation scheme, the bit error rate (BER) of the communication system can be expressed as[10]

$$\mathrm{BER} = Q\left(\frac{x_1 - x_2}{\sqrt{2N_0}}\right), \tag{4}$$

where x_1 and x_2 are the signal amplitudes at the demodulator in the first and second halves of the bit interval, respectively, and $N_0 = \sigma^2_\mathrm{shot} + \sigma^2_\mathrm{amp}$ is the total noise density. We turn "on" the LED traffic light inthe first half and turn it "off" in the second half. As a result, we obtain $x_1 = \gamma L_\mathrm{L} P_\mathrm{t} T_\mathrm{r} \sqrt{1/R_\mathrm{b}}$ and $x_2 = 0$, where γ is the responsivity of the photodiode, L_L is the path loss of the channel given by Eq. (3), P_t is the transmitting power, T_r is the transmittance of the optical bandpass filter, and R_b is the data rate.

Basing from Eqs. (3) and (4), we can determine the

relation between the data rate R_b and range D as

$$D = \sqrt{\frac{C\gamma P_t T_r}{Q^{-1}(\mathrm{BER})\sqrt{2N_0 R_b}}}. \quad (5)$$

The datasheet of the vendor indicates that the equivalent input noise density of the adopted preamplifier can be expressed as $\sigma^2_{amp} = 2pA{\cdot}\mathrm{Hz}^{-\frac{1}{2}}$.[11]. The measurement results on the background solar radiation (Fig. 2) show that the average noise density level of 2.3 μW/nm gains 3.25 for the green light optical bandpass filter with 40-nm bandwidth, 0.64 transmittance, and convex lens. The total received solar radiation power is 195 μW. Figure 4 shows the obtained range-rate tradeoff performance. At a BER of 10^{-3}, a data rate of 1 Mbps can be achieved at the range of 50 m, but it reduces to 1 kbps at 280 m.

Figure 5 shows the effect of background solar radiation noise level on the range-rate tradeoff performance, in which the noise densities are 0, 2.3, 5.4, and 140 μW/nm at a system BER of 10^{-3}. Zero solar radiation represents the night scenario, 140 μW/nm is the worst case where direct vertical irradiance from the sun is present, and the other two values represent cases with dominant horizontal diffuse irradiance. A data rate of 1 kbps can be achieved at the range of 100 m even in the worst case. The range is extended to 430 m in the best case.

Figure 2 shows that the solar radiation noise level varies with the time of the day. The solar radiation noise level is relatively small in the morning and early evening, but it is high at noon. The BER results versus the time of the day are shown in Figs. 6 and 7 to demonstrate the effect of background solar radiation variation on communication performance. Either the range or data rate is fixed.

Table 1. Parameters in the Performance Evaluation

Parameters	Value
Photodiode Active Receiving Area (cm^2)	1
Convex Lens Gain	3.25
Receiver Front-end FOV (deg.)	15
Photodiode Responsivity at 500 nm	0.28
Photodiode Responsivity at 590 nm	0.37
Photodiode responsivity at 620 nm	0.4
Traffic Light Height (m)	5
Receiver Rront-end Height (m)	1

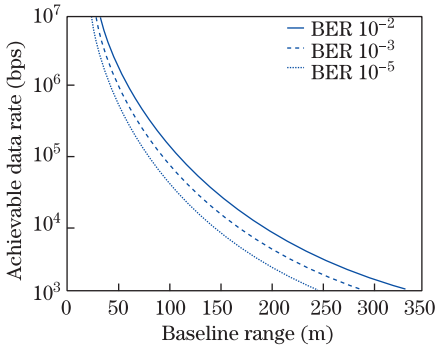

Fig. 4. Range-rate tradeoffs for different BERs.

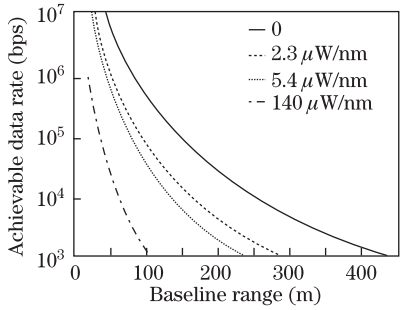

Fig. 5. Range-rate tradeoffs with different background solar radiation levels.

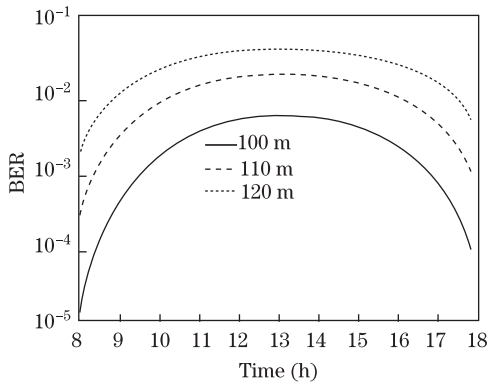

Fig. 6. BER versus time for different ranges (data rate: 100 kbps).

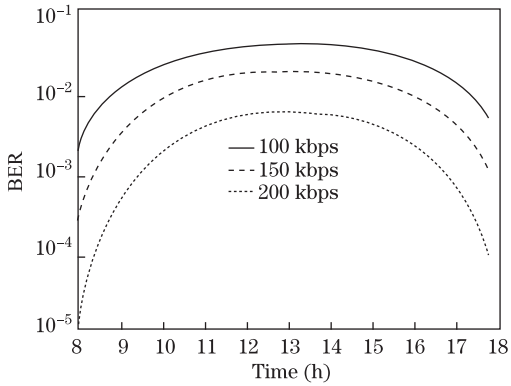

Fig. 7. BER versus time for different data rates (range: 100 m).

Three different color lamps (green light at center wavelength 500 nm, yellow light at center wavelength 590 nm, and red light at center wavelength 620 nm) with the same transmitting power level are used to compare range-rate performances. We assume that the three different optical bandpass filters have the same bandwidth of 40 nm and transmittance of 0.64. The average received solar radiation power for the optical bands are 195 μW for the 500-nm band, 530 μW for the 590-nm band, and 360 μW for the 620-nm band. Figure 8 shows the evaluated results on communication performance. The range-rate performance minimally decreases with the increased

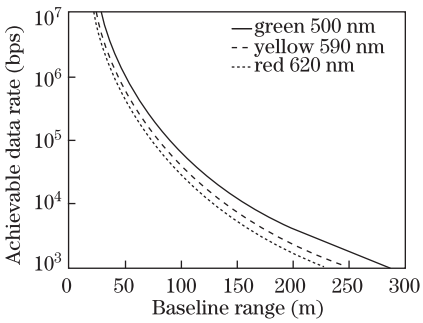

Fig. 8. Range-rate tradeoffs for three optical bands.

wavelength. Furthermore, the change in color does not significantly affect the communication performance of the system.

In conclusion, we evaluate the range-rate performance of the communication system between LED traffic lights and vehicles. The measurement results for both background solar radiation and path loss are presented, and empirical models are also proposed. Then, system performance is predicted under different conditions. Even in the worst case where the sun is within the receiver FOV, communication with a relatively high data rate (100 kbps) is still achieved in a short range (30 m). Under ordinary scenarios where only horizontal diffuse solar radiation exists, the communication range can be 100 m with a data rate of 100 kbps. We also examine the performance variation within a day (with different solar radiation levels) and the range-rate tradeoffs with three light colors. No significant difference exists in the three optical bands when all other parameters are similar. All results obtain in this study are significant for practical applications.

This work was a part of the programs, "Technology and Applications of Visible Light Communication with LEDs" and "Application Study for LED Informationization Technology," which were both supported by the Scientific Development and Innovation Collection Fund of Shenzhen.

References

1. M. Akanegawa, Y. Tanaka, and M. Nakagawa, IEEE Trans. Intell. Transp. Sys. **2,** 197 (2001).
2. P. Xu, C. Xia, F. Wu, X. Li, Q. Sai, G. Zhou, and X. Xu, Chin. Opt. Lett. **10,** 021601 (2012).
3. Z. Liu, P. Liu, and F. Yu, Chin. Opt. Lett. **10,** 112201 (2012).
4. S. Okada, T. Yendo, T. Yamazato, T. Fujii, M. Tanimoto, and Y. Kimura, in *Proceedings of IEEE Intelligent Vehicle Symposium.* 1033 (2009).
5. N. Kumar, L. N. Alves, and R. L. Aguiar, in *Proceedings of Wireless VITAE* 798 (2009).
6. I. E. Lee, M. L. Sim, and F. W. L. Kung, IET Optoelectron **3,** 30 (2009).
7. S. Iwasaki, C. Premachandra, T. Endo, T. Fujii, M. Tanimoto, and Y. Kimura, in *Proceedings of Intelligent Vehicle Symposium* 13 (2008).
8. H. Chinthaka, N. Premachandra, T. Yendo, T. Yamazato, T. Fujii, M. Tanimoto, and Y. Kimura, in *Proceedings of the 2009 IEEE Intelligent Vehicle Symposium.* 179 (2009).
9. K. Cui, G. Chen, Z. Xu, and R. D. Roberts, in *Proceedings of 2010 7th International Symposium on Communication Systems Networks and Digital Signal Processing (CSNDSP)* 621 (2010).
10. M. D. Audeh and J. M. Kahn, in *Proceedings of SUPERCOMM/ICC 2* 660 (1994).
11. K. Cui, G. Chen, Z. Xu, and R. D. Roberts, Appl. Opt. **51,** 6594 (2012).